13. COPERNICAN SYSTEM

FIGURE 13.1 (OVERLEAF).—Fresh, sharp-textured Copernican crater Aristarchus (40 km, 24° N., 47° W.). Orbiter 5 frame M–198.

13. COPERNICAN SYSTEM

CONTENTS

INTRODUCTION

Most early astronomic and geologic observers who carefully studied the Moon realized that rays are the youngest lunar features because they are superposed on all other terrains. The stratigraphically minded geologists Shoemaker and Hackman (1962) furthermore knew that the rays' youth indicates that the topographically expressed ejecta blankets of the source craters are also among the Moon's youngest. They accordingly established the Copernican System as the Moon's youngest assemblage of rock units.

No formal definition of the base of the Copernican System exists because no extensive stratigraphic-datum horizons exist near the lower system boundary. The rays of Copernicus are good early Copernican markers, but Copernicus does not mark the base of the system; many craters traditionally mapped as Copernican are older. The young, Eratosthenian mare lavas in Mare Imbrium and Oceanus Procellarum are near, but evidently not exactly at, the base of the system. Chapter 12 and table 12.1 give tentative crater-frequency and D_L criteria for dividing Eratosthenian and Copernican units, but these criteria, also, are not definitive. This chapter further specifies the position of the system's base. The end of the Copernican Period is defined as the present; a crater formed today would be Copernican.

Copernican craters are sparsely scattered over the entire Moon; Copernican mare units are concentrated in northwestern Oceanus Procellarum (pl. 11). There are half as many craters larger than 30 km in diameter as in the Eratosthenian System (44 versus 88; pls. 10, 11), and still fewer than in older time-stratigraphic units. The rays, however, make the Copernican System more conspicuous than the number of its units would indicate. Some Copernican deposits are beautifully fresh (figs. 13.1, 13.2; table 13.1). They serve as analogs of more degraded features and hint at the hidden complexity of the older rock record. In other words, as in terrestrial geology, we can say that the present is the key to the past—if the lunar "present" means hundreds of millions of years.

CRATER MATERIALS

Rays and extreme topographic freshness remain the principal criteria for the assignment of a Copernican age to craters (table 13.1). In favorable circumstances, ages are assigned more rigorously. Superposition of a given unit on the rays of Copernicus establishes its Copernican age (fig. 7.4; table 7.2). Crater counts can correlate a few units with Copernicus or with other bright-rayed craters that also are certainly Copernican (figs. 12.4, 13.3; Neukum and König, 1976; Guinness and Arvidson, 1977; Young, 1977). Blocky ejecta and other features detectable at high resolutions that are used as age criteria by Trask (1969, 1971) distinguish small Copernican craters (see chap. 7; figs. 7.12–7.14, 13.2).

Problems in distinguishing Copernican from Eratosthenian craters arise when the craters are older than Copernicus, do not contact Copernicus, are faintly rayed, or are poorly photographed. D_L values and crater frequencies (figs. 12.4, 12.8; tables 12.1, 12.3) can be determined only on superior photographs (fig. 13.4); even the best nearside

TABLE 13.1.—*Representative Copernican craters*

[Cross rules divide diameter ranges mapped differently in plate 11: smaller than 30 km, unmapped; 30 to 59 km, interiors mapped; 60 km and larger, exterior deposits mapped]

Crater	Diameter (km)	Center (lat)	Center (long)	Figure	Remarks
South Ray	0.8	9.2° S.	15.3° E.	9.9	See table 13.2.
North Ray	1.0	8.8° S.	15.5° E.	9.9	See table 13.2.
Linné	2.5	28° N.	12° E.	3.2A	Young.
Copernicus H	4.3	7° N.	18° W.	12.2B, 13.6	Dark-haloed.
Lansberg B	9	3° S.	28° W.	10.41	---
Messier	11	2° S.	48° E.	3.11A	Elongate.
Gambart A	12	1° N.	19° W.	13.5	---
Goddard A	12	17° N.	90° E.	4.7	Very young.
Sulpicius Gallus	12	20° N.	12° E.	5.16	---
Dawes	18	17° N.	26° E.	11.13	See figure 12.4.
Dionysius	18	3° N.	17° E.	10.38	Young.
Lichtenberg	20	32° N.	68° W.	10.2, 13.7	Rim flooded.
Pytheas	20	21° N.	21° W.	3.40	See table 7.2.
Thebit A	20	22° S.	5° W.	7.7	---
Conon	22	22° N.	2° E.	10.7, 10.14	---
Giordano Bruno	22	36° N.	103° E.	9.28	Very young.
Mösting	25	1° S.	6° W.	7.7	See figure 12.4.
Triesnecker	26	4° N.	4° E.	6.20	---
Proclus	28	16° N.	47° E.	3.33, 9.11, 9.15	Young; asymmetric rays.
Kepler	32	8° N.	38° W.	8.10	Young (see tables 7.2, 12.3).
Petavius B	33	20° S.	57° E.	13.4	Young (see fig. 12.4).
Godin	35	2° N.	10° E.	10.16	See table 12.3.
Autolycus	39	31° N.	2° E.	1.6, 1.7, 2.5B	Do.
Aristarchus	40	24° N.	47° W.	5.12, 7.4, 13.1	Young (see figs. 12.4, 13.3; tables 7.2, 12.3).
Olbers A	43	8° N.	78° W.	10.3	Young.
Crookes	49	10° S.	165° W.	9.21	---
Anaxagoras	51	73° N.	10° W.	3.34, 10.15	---
Aristillus	55	34° N.	1° E.	1.6, 1.7, 2.5B	See table 12.3.
Taruntius	56	6° N.	47° E.	6.13B, 6.18, 9.3	Floor uplifted.
Eudoxus	67	44° N.	16° E.	1.7, 10.12	See figure 12.4; table 12.3.
King	77	5° N.	121° E.	1.2, 3.23, 3.32, 3.36	Farside example.
Tycho	85	43° S.	11° W.	1.1, 1.8, 2.3, 3.2D	Young (see figs. 12.4, 13.3; tables 12.3, 13.2.
Copernicus	93	10° N.	20° W.	1.1, 1.6, 3.4, 3.30, 3.35, 7.4, 12.2, 13.10	Typical (see figs. 12.4, 13.3; tables 7.2, 12.3, 13.2.

Lunar Orbiter 4 H-frames are barely adequate to date Copernican crater units. Because the D_L method is valid only on level surfaces, the only crater materials it can date reliably are impact-melt pools, which are relatively small. The traditional criteria of ray brightness and topographic freshness are also hard to apply in poorly photographed areas, particularly on most of the farside poleward of lat 40° N. and lat 40° S. (pl. 2). Some observational bias may account for the excess of nearside over farside craters mapped in plate 11 (26 versus 18) and the excess of northern- over southern-hemisphere craters on the nearside (17 versus 9). Nevertheless, the identification, during two separate iterations, of half as many Copernican as Eratosthenian craters in two size ranges (min 10 km diam [see chap. 12] and min 30 km diam [pls. 10, 11]) suggests that the criteria have been consistently applied and correctly discriminate ages to a good approximation.

Copernican craters can commonly be identified by remote sensing. Temperatures measured in the infrared during a total lunar eclipse or from orbit are valuable for detecting young blocky craters and other fresh surfaces covered by little insulating fragmental material (see chap. 5, subsection entitled "Other Properties"). The eclipse infrared values were extensively used during the lunar geologic-mapping program before the advent of spacecraft photography to distinguish between Copernican ("hot") and Eratosthenian ("cool")

craters (fig. 13.5). Some of the crater-age assignments in this volume still rest on this distinction (for example, Agrippa and Godin, fig. 10.16). Radar has also been used to detect blockiness in craters and thus to estimate cohesiveness and age-related state of degradation (Thompson and others, 1980, 1981). Color spectra may also reveal youthful surfaces in craters; enhanced reflectivity near 1 and 2 μm indicates high proportions of fresh crystalline material to agglutinitic glass, whose formation is a function of exposure age (see chap. 5). Color contrasts seen on color-difference images also are strongest around the youngest craters (fig. 5.20).

Age interpretations of low albedo have changed for crater materials as they have for mare materials. The dark color of the volcanic maria and the existence of the irregular, dark-haloed endogenic craters in Alphonsus (fig. 5.10*F*) led to volcanic interpretations for the dark halos of certain circular craters as well (Shoemaker and Hackman, 1962, p. 297; Shoemaker, 1964; Salisbury and others, 1968). Impact origin was also entertained for these dark-haloed circular craters (Carr, 1965b) and was later substantiated by the impactlike morphology (deep floor, rough ejecta) of a typical example, Copernicus H (figs. 12.2*B*, 13.6). Most circular craters with impactlike morphology and dark ejecta are superposed on bright rays or other thin bright materials that, in turn, overlie maria or dark terra plains (see chap. 9; figs. 13.5, 13.6). Thus, the halos are only dark by contrast with their surroundings and probably contain basaltic materials brought to the surface by impacts (Scott and others, 1971, p. 276–277; Lucchitta, 1972; Hodges, 1973a; Lucchitta and Schmitt, 1974; Wolfe and others, 1975; Schultz and Spudis, 1979). Whereas the interiors of most endogenic craters are dark, the interiors of dark-haloed impact craters are as bright as those of any other impact crater. The dark-haloed craters superposed on Copernican rays are, of course, Copernican.

Other strong contrasts in albedo may also indicate youth because albedos become neutral with advancing age (see chap. 5). The rim of the young crater Tycho is surrounded by both bright and dark zones (fig. 1.1), which are unobserved around most craters. Dark and bright rays were artificially generated by impacts of spacecraft on the Moon (Whitaker, 1972a) and presumably also surrounded many natural

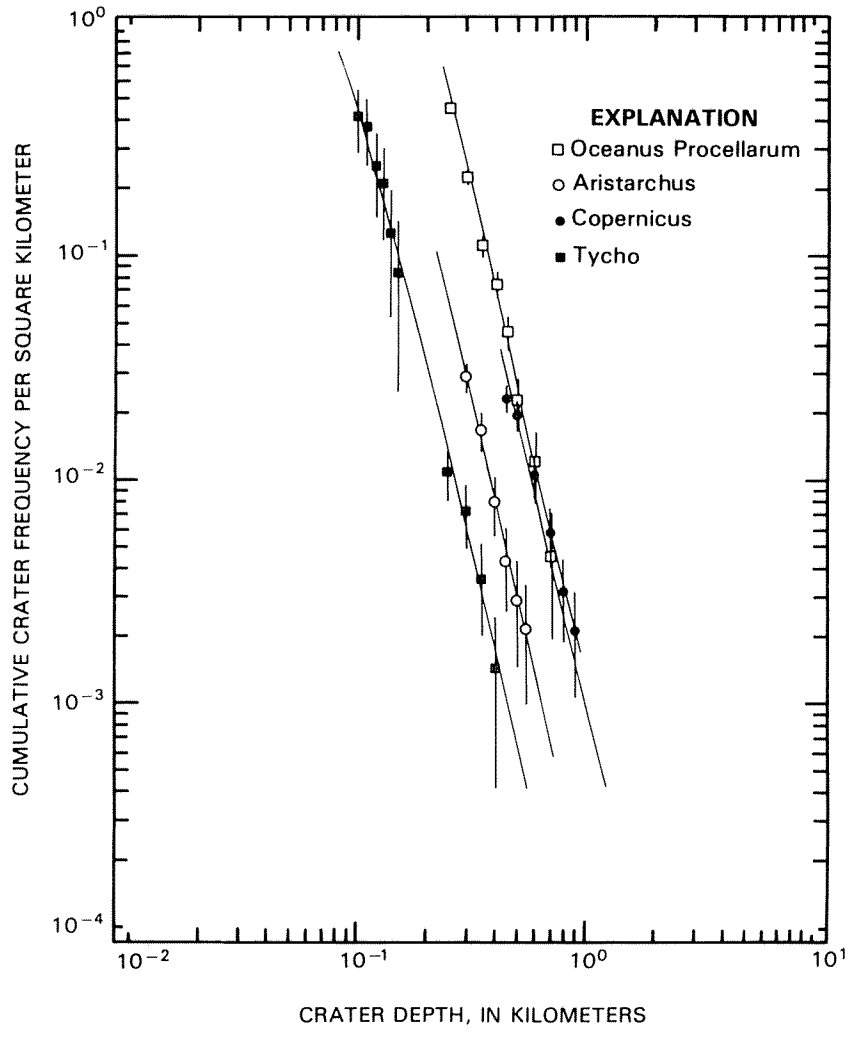

FIGURE 13.3.—Frequencies of craters superposed on three Copernican craters, in comparison with mare units in Oceanus Procellarum shown in figure 12.3 (compare fig. 12.4*A*). Courtesy of Gerhard Neukum.

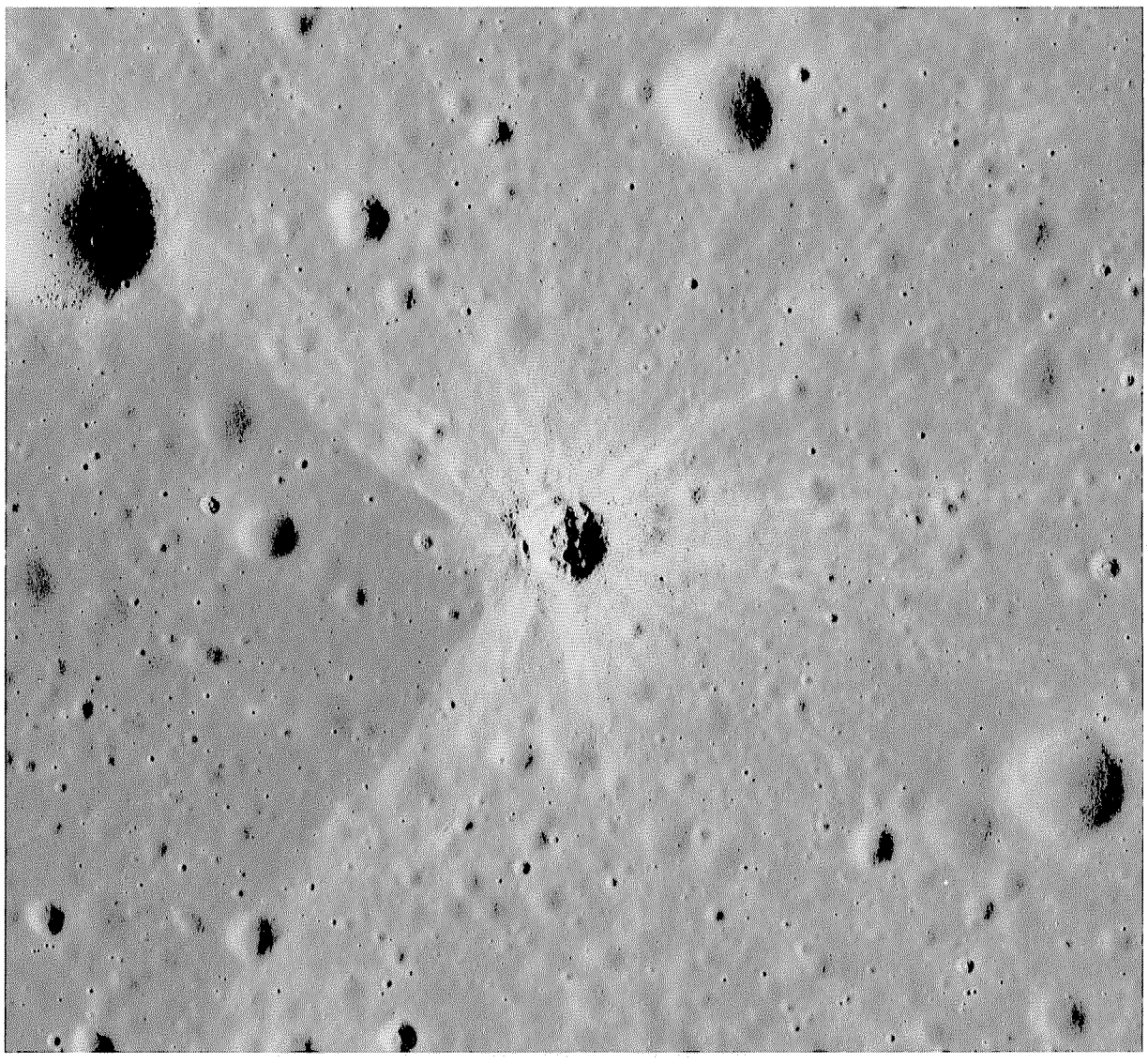

FIGURE 13.2.—Fresh Copernican crater, about 0.5 km in diameter, in central Mare Serenitatis. Blocks ejected from crater in direction of bright rays are preserved as far as three crater diameters from rim. In contrast, blocks are preserved only in interior and on rim crest of older, larger crater in upper left. Mare surface is brightened by Copernican rays except in sector of nondeposition left of crater (probably owing to oblique impact). Apollo 15 frame P–9337.

impacts, but most have been homogenized. Original albedos of target strata uplifted in the crater may be preserved in some young craters (fig. 3.29).

In summary, the brightest rays, most highly contrasting albedos of other crater materials, highest thermal anomalies, freshest morphologies, most coherent ejecta blocks, deepest floors, and fewest superposed craters indicate a Copernican crater age. The relative degree of development of these attributes also may be used to subdivide the Copernican System (Trask, 1969, 1971; Wilhelms and McCauley, 1971). Mapping and dating of older craters is aided by reference to the appearance of Copernican primary and secondary craters.

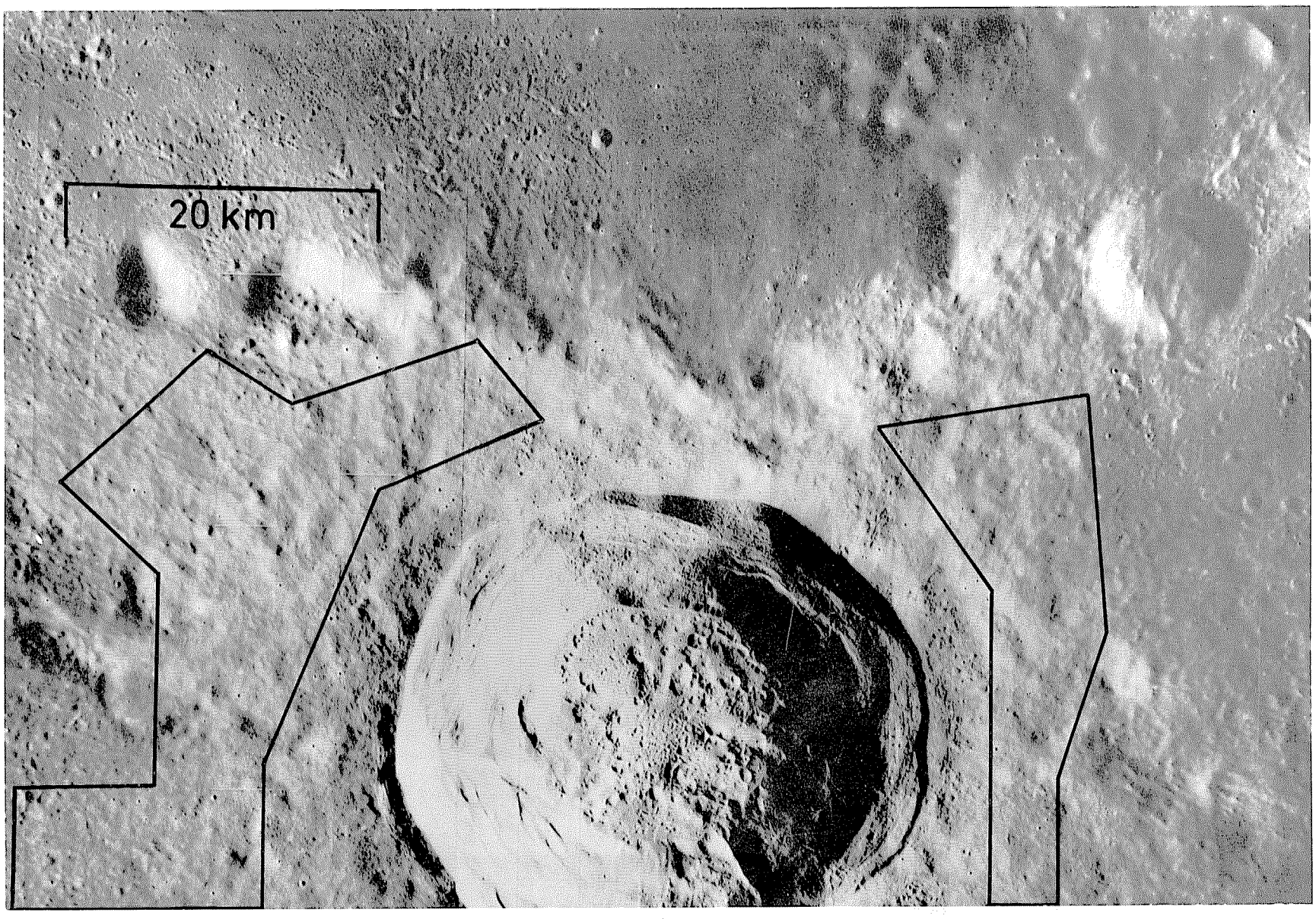

A

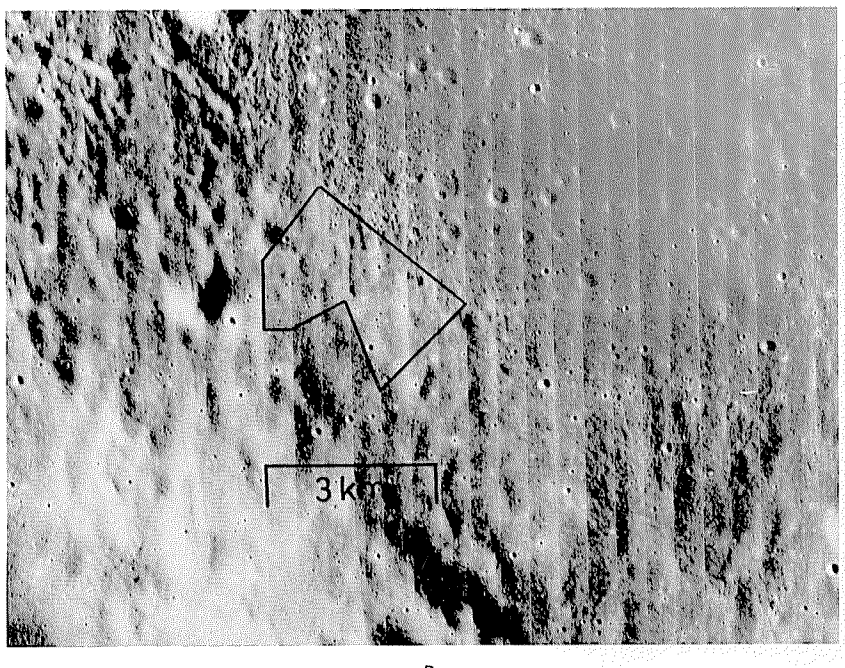

B

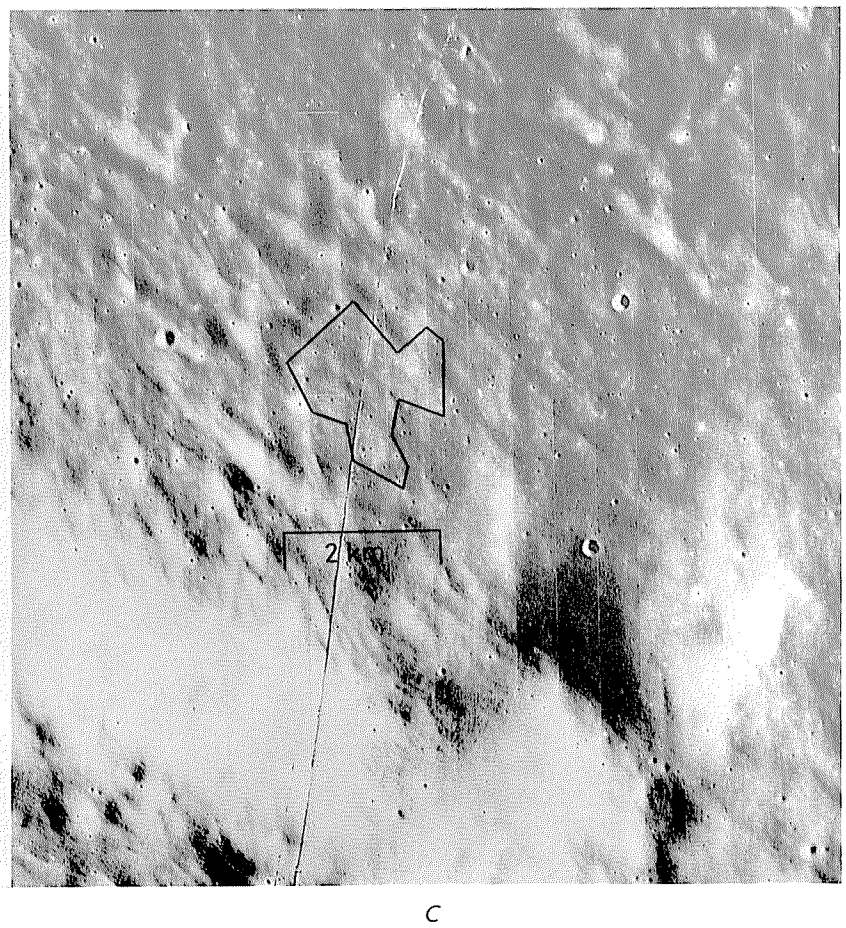

C

FIGURE 13.4.—Fresh Copernican crater Petavius B (33 km, 20° S., 57° E.), illustrating crater counts made on small areas from superior photographs. Counts made at each scale are combined and included in figure 12.4. Courtesy of Gerhard Neukum.

A. Regional view. Ejecta is indistinct in north sector because it is superposed on mare material and probably because of oblique primary impact. Orbiter 4 frame M–37.

B. Near northern "excluded zone." Orbiter 5 frame H–37.

C. Southeast sector. Orbiter 5 frame H–37.

FIGURE 13.5.—Small dark-haloed craters (arrows) superposed on rays of Copernican crater Gambart A (12 km), a thermal-infrared "hotspot." Mare material underlies Gambart A. Apollo 12 frame H–7737.

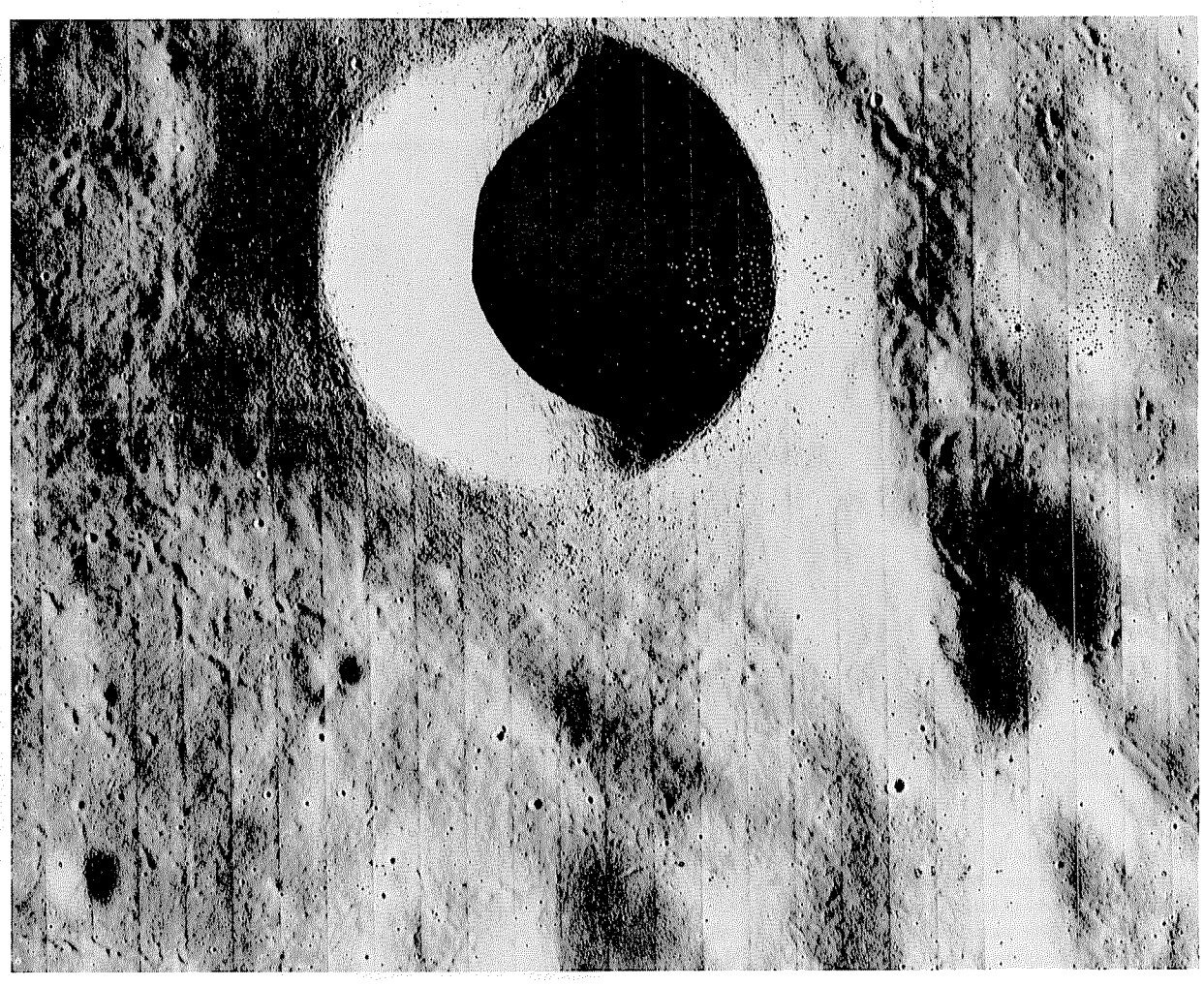

FIGURE 13.6.—Dark-haloed crater Copernicus H (4.3 km; compare fig. 12.2*B*), showing subconcentric dunes characteristic of small impact craters. Orbiter 5 frame H–147.

MARE MATERIALS

Northern Oceanus Procellarum contains some very young mare materials (pl. 11), the largest patch of which covers the southeastern ejecta of the bright-rayed crater Lichtenberg (fig. 13.7; Moore, 1967; Wilhelms, 1970b). Thus, the mare basalt is Copernican, and the Copernican Period had started by the time it was extruded. Three additional patches that I estimate to have the same or lower frequencies as this post-Lichtenberg unit are also mapped in plate 11. This part of northern Oceanus Procellarum was apparently the most active, or only, site of Copernican volcanism.

Dating of these patches would greatly help in determining the duration of lunar volcanism. The density of craters superposed on the patch near Lichtenberg has been determined to be about equal to that on Copernicus (P.H. Schultz and P.D. Spudis, written commun., 1982). If, as discussed previously, a given impact superposes a larger crater on breccia than on basalt, the cumulative size-frequency curve for a crater deposit will be displaced upward from that for a mare deposit of the same age (see chap. 12; fig. 12.4; tables 7.1, 12.1; Schultz and Spencer, 1979; Ahrens and Watt, 1980). The flow that embays Lichtenberg would thus be younger than Copernicus.

The smallest D_L value determined by Boyce and others (1975), 150 ± 20 m, probably pertains to one of the Copernican patches. This value is somewhat smaller than 165 ± 25 m, the D_L value for the extensive neighboring Eratosthenian flows.

The small Copernican mare units are among the spectrally bluest on the color-difference photograph reproduced in figure 5.20. They are slightly bluer than the adjacent Eratosthenian units, whose spectral class is hDSA (pl. 4); the Copernican units are too small to show in plate 4 or on the spectral map of Pieters (1978). These units overlie the extensive Eratosthenian flows in the middle trough of the Procellarum basin (pl. 10). Other Copernican mare units may eventually be found in maria superposed on the central Procellarum basin, for example, Mare Imbrium; or young magmas melted there may not have been able to rise through the thick section of Imbrian and Eratosthenian basalt already present.

Otherwise, no Copernican volcanic materials are known. Dark-mantling materials that were thought to be young on the basis of smoothness have been proved to be Imbrian in age (see chap. 11). Volcanism or emissions of gas were among the early-suggested explanations for Reiner gamma (fig. 12.10; McCauley, 1967b) and similar but more extensive bright "swirls" on the farside (fig. 4.7; El-Baz, 1972). Some connection with lunar magnetism and an origin by Copernican (Schultz and Srnka, 1980) or pre-Copernican (Hood and others, 1979) impacts have been suggested more recently (see chap. 10, section entitled "Imbrium-Secondary Craters," and chap. 12, section entitled "Crater Materials").

STRUCTURE

Copernican tectonism was minor. Narrow gashes in the mare west of the Apollo 17 landing site (fig. 13.8) are young but probably resulted from drainage of regolith into older voids (B.K. Lucchitta, in Masursky and others, 1978, p. 209). The existence of mascons indicates that isostatic compensation of mare-filled basins has ceased or is very sluggish. Continuing subsidence and the resulting mare-ridge compression (see chap. 6) are unlikely because most endogenic moonquakes do not correlate with maria (Nakamura and others, 1979, fig. 3; Solomon and Head, 1979). The only definite Copernican tectonic features are the uplifted floors of such craters as Taruntius (fig. 6.13*B*). Binder (1982), however, suggested that young-appearing lobate scarps on the farside terra (Masursky and others, 1978, p. 96) are thrust faults caused by currently increasing global contraction.

Lunar seismic energy of endogenic origin is minuscule, only 10^{-12} to 10^{-7} that of the Earth (French, 1977, p. 228; Lammlein, 1977, p. 266). The most energetic, but rarest, endogenic moonquakes probably originate in the upper mantle from small thermal stresses (Nakamura and others, 1979). The most common, but very small, moonquakes originate at depths of $1{,}000 \pm 100$ km from tidal stresses that do not deform the surface (Lammlein, 1977). The third type of moonquake, intermediate in frequency but unlimited in magnitude, is induced by impacts.

CHRONOLOGY

Establishing the chronology of the Copernican Period is hindered by the small number of well-dated stratigraphic units of regional extent. At 1.29 aeons old (Bernatowicz and others, 1978), sample 15405 from the Apollo 15 landing site is the youngest rock-size lunar sample and the oldest that could be Copernican (fig. 13.9; table 13.2). This sample contains KREEP-rich "granitic" and "monzodioritic" material (Ryder and others, 1975a; Ryder, 1976) that is exotic to the landing site. A source in the Copernican craters Aristillus or Autolycus, centered 250 and 150 km north of the landing site, respectively, is considered possible by most investigators. Autolycus is marginally favored for several reasons: (1) It formed at least partly on the required target, KREEP-rich plains (Metzger and others, 1979), whereas mare basalt probably constitutes the uppermost target material of Aristillus; (2) it is closer than Aristillus to the collection site, easing somewhat the objection that the 1-m boulder from which sample 15405 was taken should have disintegrated in a long flight; and (3) it is older than Aristillus, making it the more likely source of 1.29-aeon-old material if Aristillus is younger than Copernicus (as tentatively suggested by Guinness and Arvidson, 1977) and if Copernicus is about 0.8 aeon old.

Most estimates of the post-Imbrian cratering rate are based on an 0.8- to 0.85-aeon age for Copernicus that was determined on light-colored KREEP-rich material dug from a shallow trench in the Apollo 12 mare regolith (Hubbard and Gast, 1971; Hubbard and others, 1971; Marvin and others, 1971; Meyer and others, 1971). This material was identified with Copernicus by the situation of the landing site along a Copernicus ray (fig. 13.10; Pohn, 1971) and by the fact that part of the Copernicus target material was the KREEP-rich (see chap. 10) Fra Mauro Formation (Schmitt and others, 1967). U-Pb-Th systematics yielded a date of 0.85 ± 0.10 aeon for a thermal event affecting regolith fragments (Silver, 1971). Although U-Pb-Th techniques have proved to be ambiguous in many lunar stratigraphic applications, the age of this event seemed to be substantiated by Ar-Ar determinations of 0.81 ± 0.04 aeon on sample 12033 (Eberhardt and others, 1973b; Alexander and others, 1976). Alexander and others (1977) obtained similar results for another KREEP-rich sample, 12032.

The identification of this approximately 0.8-aeon age with Copernicus has been doubted from several standpoints. Wasson and Baedecker (1972) doubted that primary ejecta would be preserved so far (340 km) from Copernicus. Quaide and others (1971, p. 715)

TABLE 13.2.—*Absolute ages of Copernican rock units*

[Methods: Ar-Ar, the ^{40}Ar-^{39}Ar method, applicable to old rocks (Turner, 1977). Kr-Kr, dating of duration of exposure to the space environment (exposure age) by measuring the ratio of the radioactive isotope ^{81}Kr generated by cosmic-ray spallation to stable krypton isotopes, generally ^{83}Kr; applicable to relatively recent exposures (Marti, 1967; Arvidson and others, 1975). U-Th-Pb, applicable to major re-equilibrations in old rocks; the entire system of U, Th, and Pb isotopes was examined by Silver (1971).
References: A76/77, Alexander and others (1976, 1977); B73, Behrmann and others (1973); B78, Bernatowicz and others (1978); C72, Crozaz and others (1972); D74, Drozd and others (1974); D77, Drozd and others (1977); E73b, Eberhardt and others (1973b); E77, Eugster and others (1977); LM72, Lugmair and Marti (1972); M73, Marti and others (1973); S71, Silver (1971). Summarized by Arvidson and others (1975)]

Unit	Apollo sampling site	Sample	Age (m.y.)	Method	Reference
South Ray Crater----------	16	Several	2.04±0.08	Kr-Kr	D74
Shorty Crater----------	17	do.	19	Kr-Kr	E77
Cone Crater----------	14	14306 (dark)	23.4±1.4	Kr-Kr	C72
		14306 (light)	25.4±2.9	Kr-Kr	C72
		14321,FM 1+2	23.8±0.6	Kr-Kr	LM72
		14321,FMS	27.2±0.5	Kr-Kr	LM72
North Ray Crater----------	16	Several	48.9±1.7	Kr-Kr	B73, M73
			50.3±0.8	Kr-Kr	D74
Tycho (bright landslide)---	17	do.	109±4	Kr-Kr	D77
Copernicus (ray)----------	12	12033	810±40	Ar-Ar	E73b
			810^{+400}_{-50}	Ar-Ar	A76/77
		Others	850±100	U-Th-Pb	S71
Autolycus or Aristillus (ray).	15	15405,90	1,290±40	Ar-Ar	B78

observed that the Copernicus ray begins at a cluster of secondary craters only 45 km north of the landing site; the samples would thus include material excavated at that point (fig. 13.10). Alexander and others (1977) pointed out that non-KREEP particles yield the same ages as the KREEP-rich samples and questioned the identity of the high-temperature event. Finally, Alexander and others (1976, 1977), though favoring the 0.8-aeon age as the more significant, showed that a plateau around 1.2 to 1.5 aeons is also quite well defined both in their data and in those of Eberhardt and others (1973b).

If the samples are not from Copernicus or if one of these older ages is that of the crater, most current estimates for the cratering rate would have to be revised. Earlier discussions in this volume suggest, however, that abandonment of the 0.8-aeon age would be premature. The argument that primary Copernicus ejecta is not present at the Apollo 12 landing site is based largely on the upper equation in figure 10.26, which is highly questionable (see chap. 10, section entitled "Fra Mauro Formation"). Spectral studies show that primary ejecta is present in rays (see chap. 3; Pieters and others, 1982). Mixtures of diverse shock grades and compositions (KREEP-rich and KREEP-poor) are the rule rather than the exception in impact deposits (see chaps. 3, 8–10). Furthermore, the secondary impacts 45 km north of the site could have reexcavated the Fra Mauro Formation (fig. 13.10) and reset its age (although resetting by secondary impacts is doubted by most investigators). In summary, the presence of 0.8-aeon-old primary Copernicus ejecta or some other influence of Copernicus on the age of the analyzed material is possible, despite the objections.

The best established date of a large Copernican crater is probably the one that appears to rest on the flimsiest evidence. The landslide at the Apollo 17 landing site was probably triggered by the impact of projectiles from crater Tycho, 2,250 km away (fig. 13.11; Wolfe and others, 1975; Arvidson and others, 1976; Lucchitta, 1977a). The duration of the landslide's exposure to cosmic rays and thus its time of formation has been accurately bracketed at 0.1 aeon (Arvidson and others, 1976; Drozd and others, 1977). Similar exposure ages of regolith materials in the central area of the landing site may date excavation by the "Central Cluster" craters (for example, Camelot and Sherlock, figs. 9.17, 11.15), which are thought to be additional Tycho secondaries (Wolfe and others, 1975, 1981; Lucchitta, 1977a). The age of Tycho is, therefore, widely accepted as about 100 million years and probably can be pinpointed to 109 million years (Drozd and others, 1977).

The three best established Copernican ages (Arvidson and others, 1975) were obtained from the exposure ages of small craters (table 13.1). Two young craters at the Apollo 16 landing site, North Ray and South Ray, are 50 million and 2 million years old, respectively. Cone Crater at the Apollo 14 landing site lies between the two, at about 25 million years (fig. 13.12). These absolute age differences are consistent with the scheme of Trask (1969, 1971; Moore and others, 1980a). Several other craters have been dated by exposure ages, including Shorty at the Apollo 17 landing site (19 million years; Eugster and others, 1977) and, less directly, West at the Apollo 11 landing site (100 million years; see chap. 11; Beaty and Albee, 1980).

FIGURE 13.7.—Crater Lichtenberg (L; 20 km), northwestern Oceanus Procellarum. Black-and-white north arrow shows same point in *A* and *B*.
A. Telescopic view suggesting sharp truncation of Lichtenberg materials by discrete dark unit.
B. Lichtenberg ejecta flooded by mare basalt (white arrow) and thinly mantled by dark-mantling material (d). Orbiter 4 frame H–170.

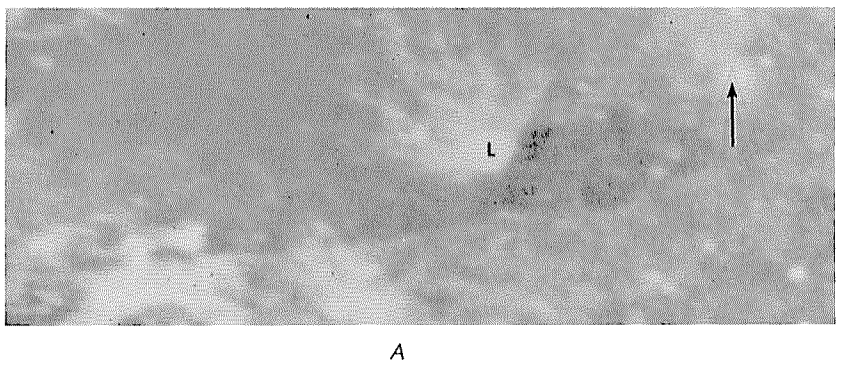

A

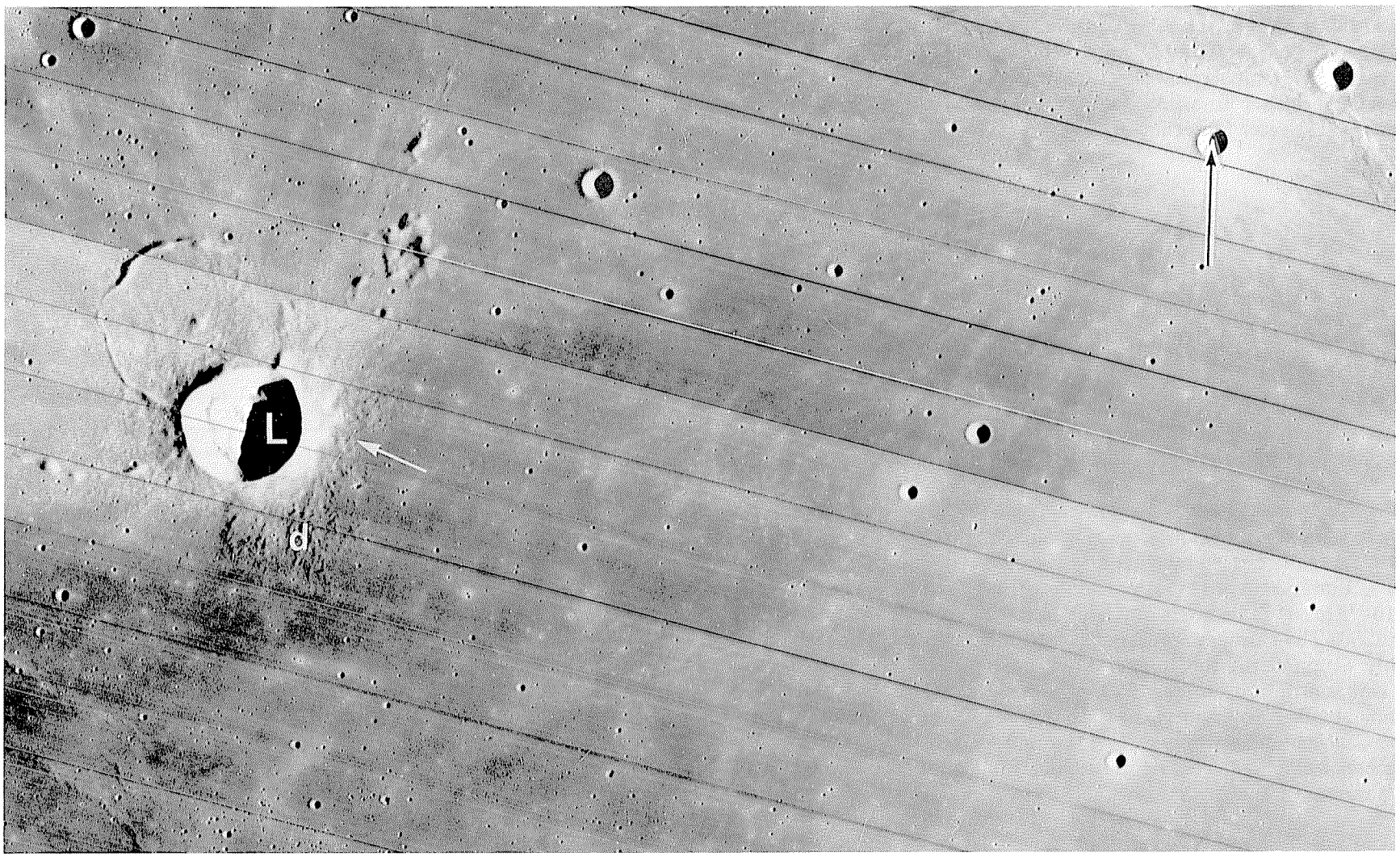

B

Because no stratigraphic units older than 0.8 or 1.29 aeons and younger than the 3.16-aeon-old Apollo 12 mare units have been absolutely dated even tentatively, the ages of the many stratigraphic units that formed during this long gap in the record must be derived by interpolation based on the cratering-rate curve (fig. 13.13). However, the shape of this curve is poorly constrained because the known ages are so widely separated and the best Copernican ages are too young to affect it significantly.

Independent knowledge of the cratering rate would provide the necessary basis for interpolation. The terrestrial cratering rate is used to calibrate the impact rate in the Earth-Moon system, with corrections for the sampling problem caused by a geologically active Earth and for Earth-Moon differences in gravity and target properties (Baldwin, 1949, 1963, 1964, 1971; Öpik, 1960; Shoemaker and others, 1962a, 1979; Hartmann, 1965b; Grieve and Dence, 1979; Grieve and Robertson, 1979; Basaltic Volcanism Study Project, 1981, chap. 8; Shoemaker, 1981). Some authors believe that the cratering rate has been constant since the Late Imbrian (Hartmann, 1972c; Soderblom and Lebofsky, 1972; Neukum and König, 1976, p. 2881; Guinness and Arvidson, 1977; Young, 1977). The shapes of the lunar and terrestrial curves suggest to others that the rate has declined during the past aeon (Trask, 1972; Soderblom and Boyce, 1972; Neukum and König, 1976, p. 2880; Shoemaker and others, 1979).

A curve corresponding to a constant rate since 3.2 aeons ago and fitted to a point between the Apollo 12 and 15 crater-frequency midpoints (curve a, fig. 13.13*A*) passes near, but not through, the bar representing the 0.8-aeon age and the frequencies of small craters superposed on Copernicus. The fit would be better if (1) the cratering rate has varied (curve b, fig. 13.13*A*), (2) the cratering rate was constant but has declined more steeply than shown because the crater

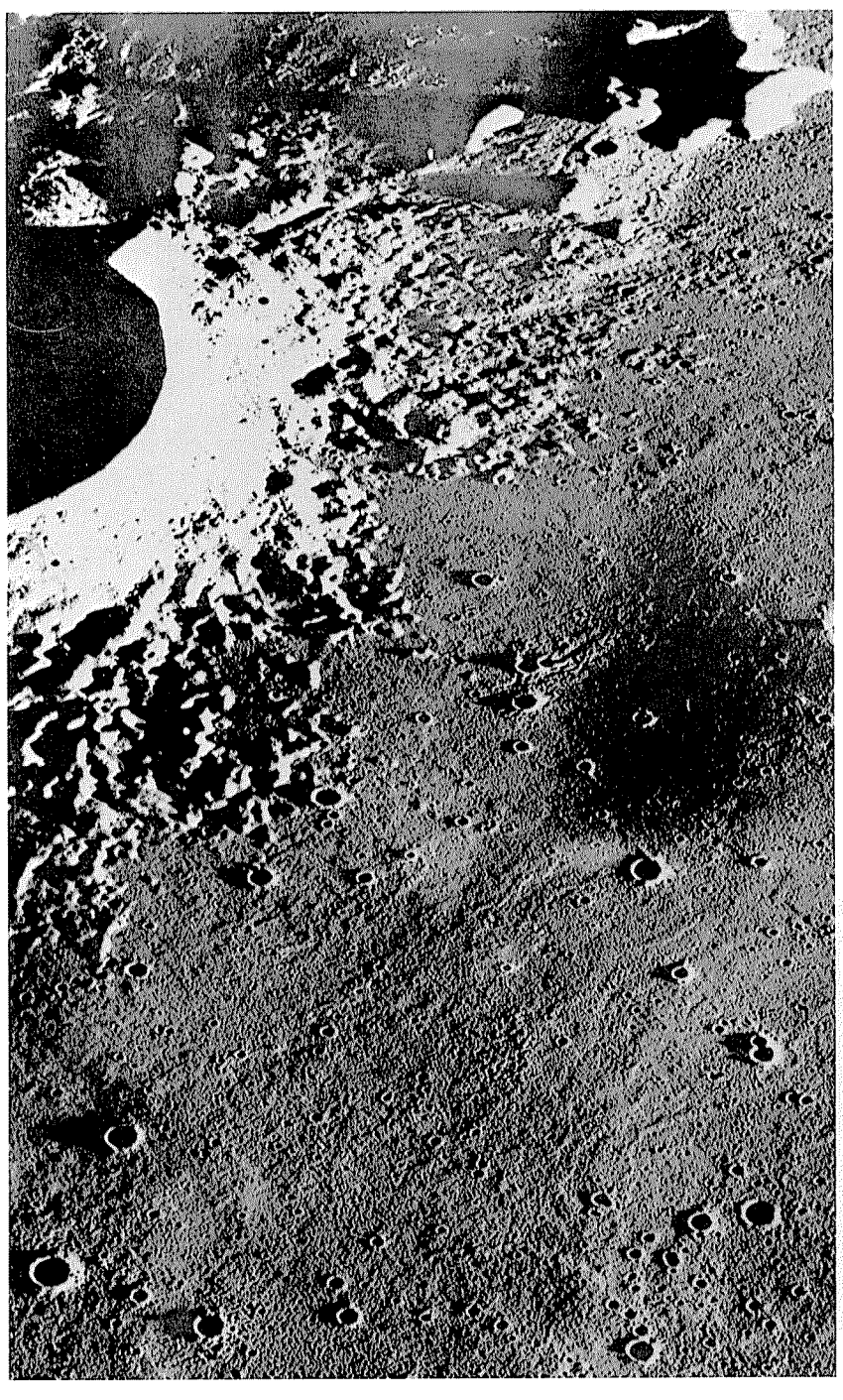

C. Detail. Apollo 15 frame P–0370.

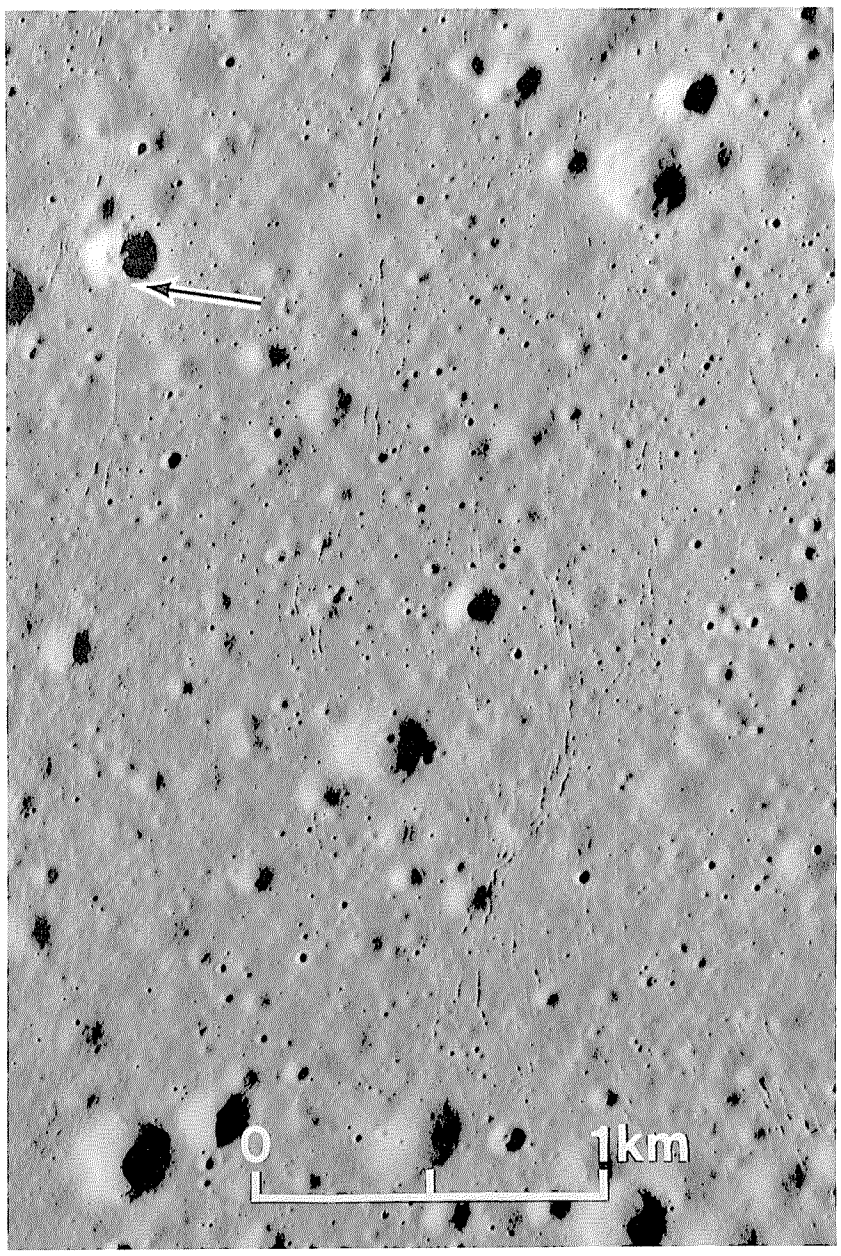

FIGURE 13.8.—Narrow gashes in surface of eastern Mare Serenitatis just west of Apollo 17 landing site. Width on the order of tens of meters and apparent transection of rim of bright blocky crater (arrow) suggest a Copernican age. Gashes probably formed by drainage of regolith into larger bedrock grabens (B.K. Lucchitta, in Masursky and others, 1978, p. 209). Apollo 17 frame P–2313.

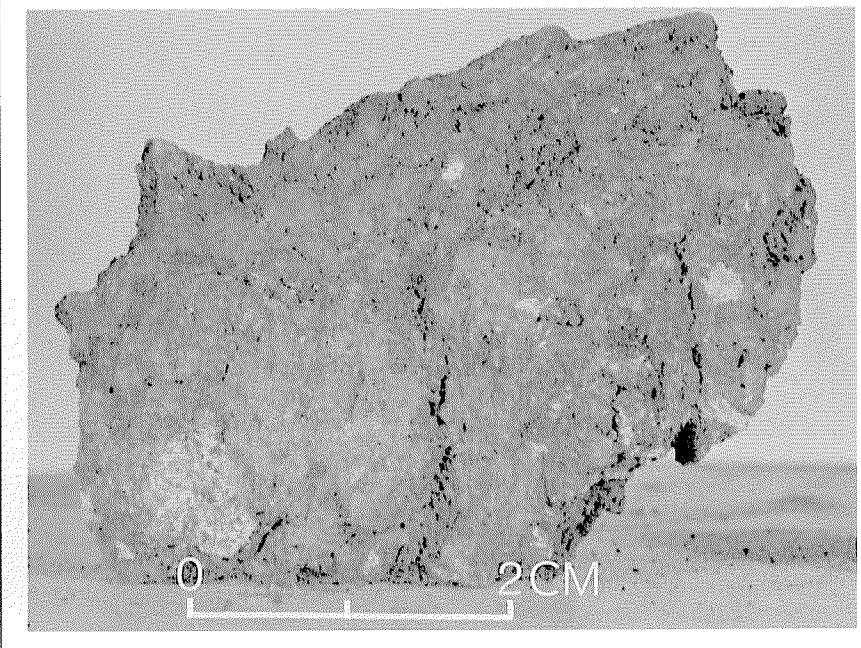

FIGURE 13.9.—Sample 15405, the youngest dated lunar rock, from Apennine front (sta. 6A), Apollo 15 landing site.

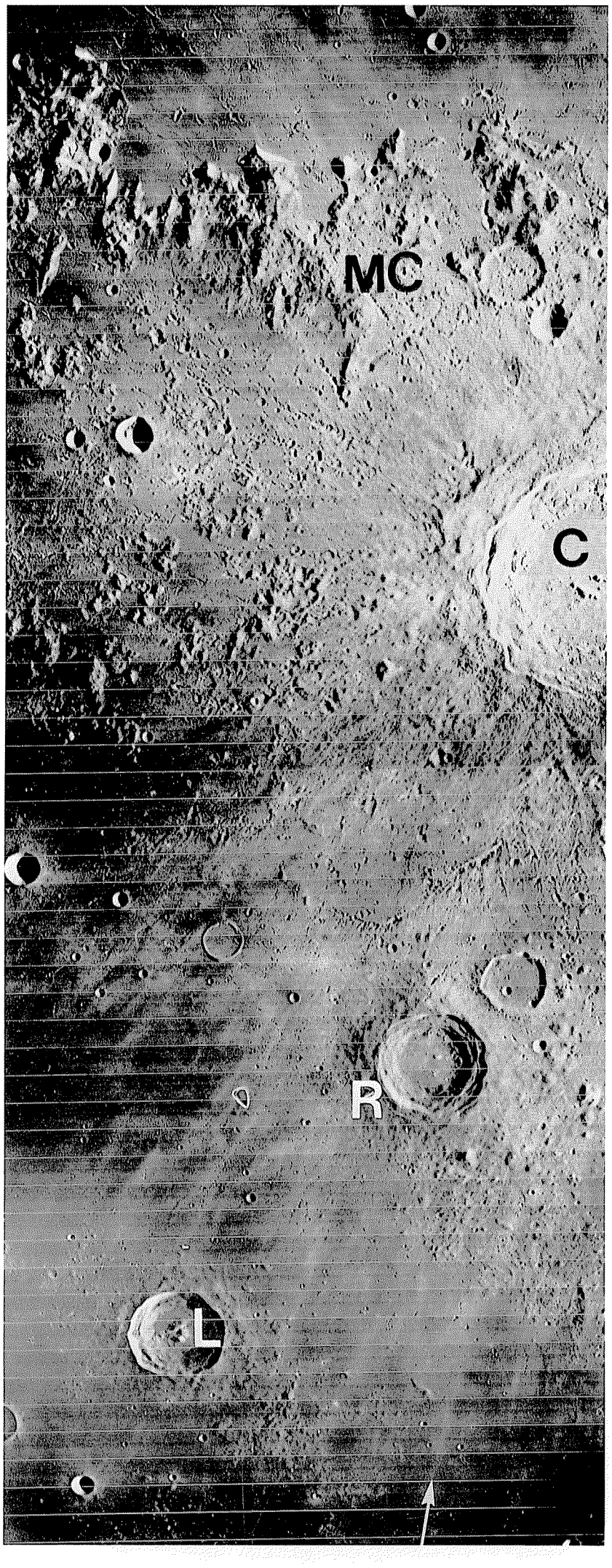

FIGURE 13.10.—North-south strip from crater Copernicus to Apollo 12 landing site.
A. Arrow indicates Apollo 12 landing site and points along ray toward Copernicus (C). Other craters include Reinhold (R; 43 km, 3° N., 23° W., probably Eratosthenian), and Lansberg (L; 39 km, 0°, 27° W., Upper Imbrian). Montes Carpatus (MC), part of Imbrium basin rim, divide Maria Imbrium (above) and Insularum (below). Orbiter 4 frame H–126.

frequencies determined for the Apollo 12 and 15 basalt units are too small (curve c, fig. 13.13*A*), (3) the crater-frequency values determined for Copernicus are too large, or (4) Copernicus is about 1.2 aeons old (point a′, fig. 13.13*A*), one of the possibilities mentioned by Alexander and others (1976, 1977). The Copernicus and Apollo 12 and 15 frequencies could be reconciled if substrate properties affect the size-frequency curves, as has been suggested. For example, if the frequency of small craters (normalized to min 1 km diam) superposed on Copernicus were about 6.5×10^{-4} per square kilometer, Copernicus would fall on the constant-rate curve, which applies to mare substrates, without any adjustment of the absolute age (point a″, fig. 13.13*A*). The D_L values could be reconciled in similar ways (fig. 13.13*B*). Because of the many uncertainties in both the absolute and relative ages of Copernicus, the currently available data appear to be equally consistent with either a constant or a varying cratering rate since 3.2 aeons ago. I tentatively accept the simpler model, the constant rate.

Granted a constant rate, wide latitude still remains in assessing the age of the Eratosthenian-Copernican boundary because of the gap in the record and the uncertain significance of the crater frequencies and D_L values. Because most assessments of the stratigraphic significance of the crater frequencies and D_L values given in this volume are based on previous calibrations with the large craters traditionally mapped as Eratosthenian or Copernican, I return to this basis for estimating the duration of the two periods. If the craters larger than 30 km in diameter mapped here (pls. 10, 11) formed at a constant rate since 3.2 aeons ago, formation of the 88 Eratosthenian and 44 Copernican craters would require 2.13 and 1.07 aeons, respectively. Similarly, the 256 Eratosthenian and 145 Copernican craters larger than 10 km in diameter mapped on the nearside by Wilhelms and McCauley (1971) (see chap. 12) would require 2.04 and 1.16 aeons, respectively. Averages of 2.1 and 1.1 aeons are tentatively adopted here for the Eratosthenian and Copernican Periods.

In summary, a 1.1-aeon duration for the Copernican Period is consistent with: (1) a constant impact rate for primary craters of all sizes since the beginning of the Eratosthenian Period 3.2 aeons ago, between the emplacement of the Apollo 12 and 15 basalt units; (2) existing age assignments of craters based on the criteria of stratigraphic superpositions, superposed craters, rays, morphology, and remote sensing; (3) a 0.8-aeon age for Copernicus; and (4) a position of Copernicus somewhat above the base of the Copernican System, in accord with stratigraphic estimates (fig. 7.1; table 7.2). Future data may demonstrate that the Copernican Period was longer or shorter than 1.1 aeons.

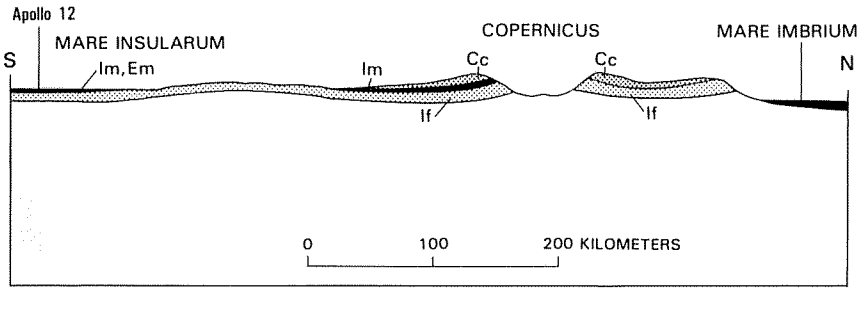

B. Geologic cross section drawn along length of *A* from base of arrow to upper right corner. Units, from oldest to youngest: If, Fra Mauro Formation; Im, Imbrian mare basalt; Em, Eratosthenian mare basalt; Cc, Copernicus ejecta. Fra Mauro Formation composes submare section from Montes Carpatus to Apollo 12 landing site and thus would be excavated by postmare craters, including Copernicus and its secondaries, anywhere along this profile.

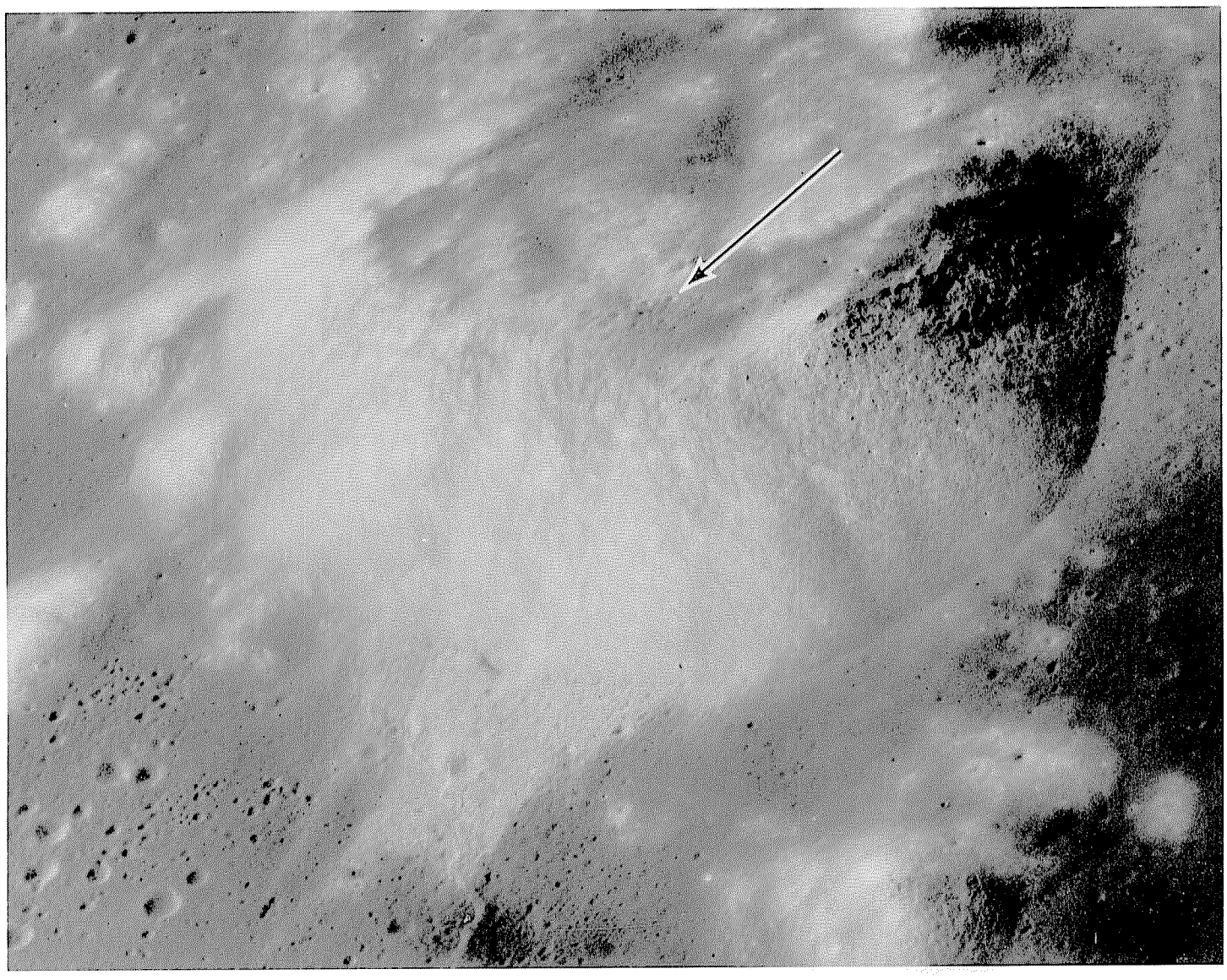

FIGURE 13.11.—Landslide (light-colored area at bottom) triggered from slope of South Massif, bordering the Taurus-Littrow Valley, by impact of projectiles from young Copernican crater Tycho, 2,200 km to southwest; arrow indicates probable Tycho secondaries (Lucchitta, 1977a). Massif is about 2,000 m high. South at top. Apollo 15 frame P–9297.

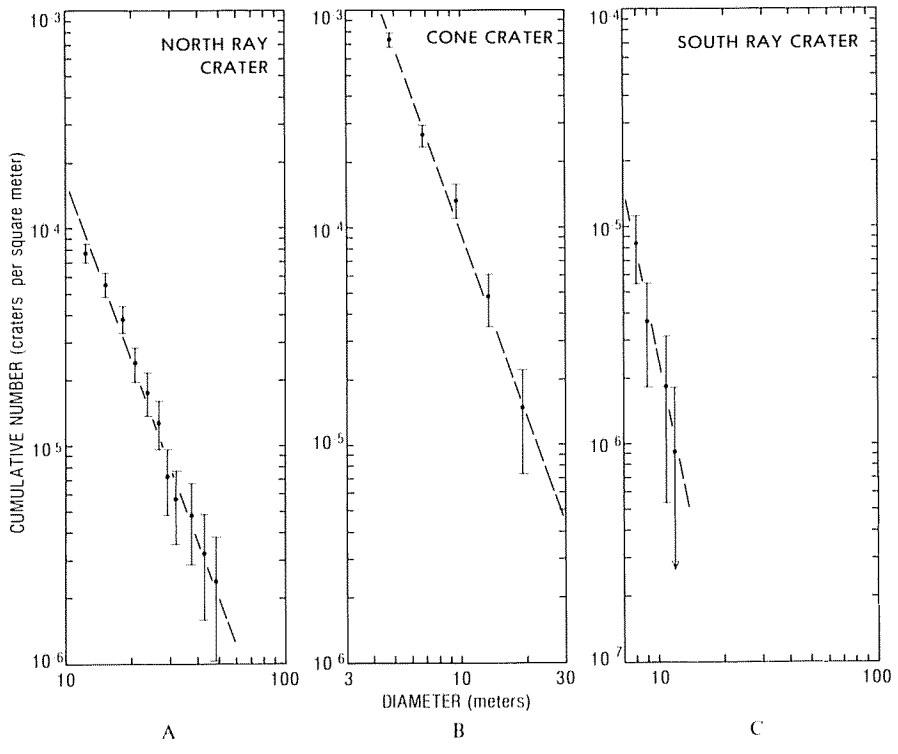

FIGURE 13.12.—Size-frequency distributions of very small craters superposed on the three sampled and absolutely dated Copernican craters, North and South Ray Craters at Apollo 16 landing site and Cone Crater at Apollo 14 landing site (Moore and others, 1980a).

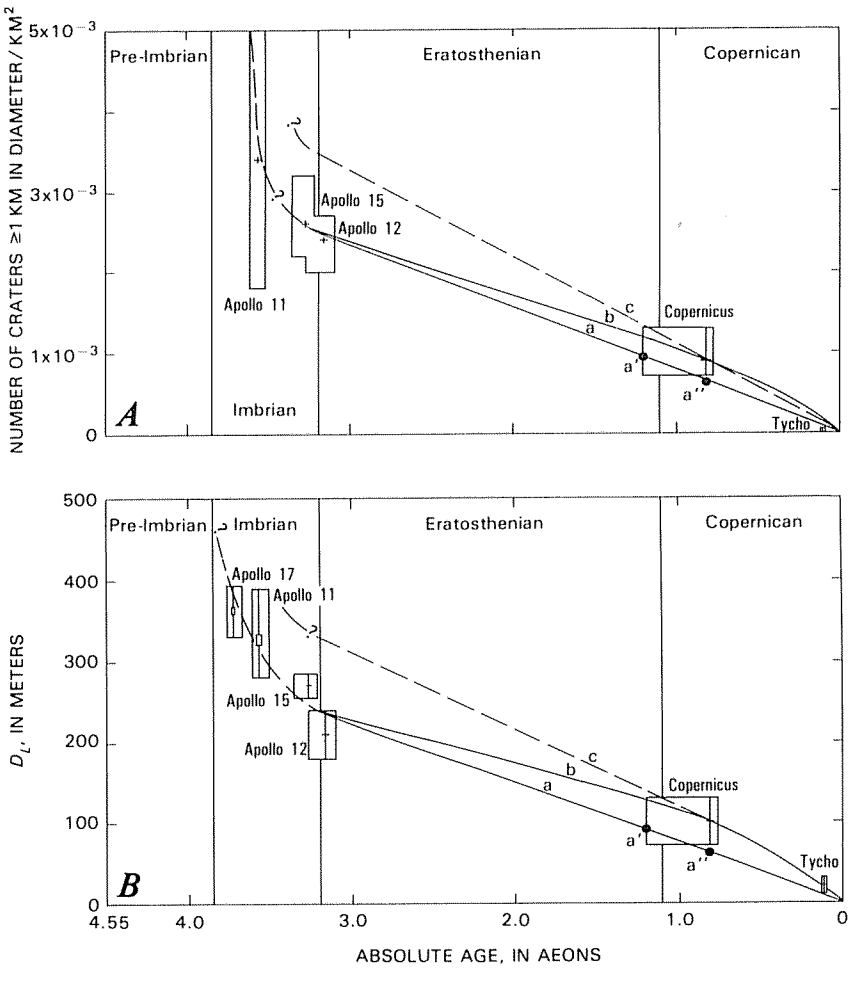

FIGURE 13.13.—Alternative cratering rates since 3.2 aeons ago. Eratosthenian-Copernican boundary is estimated from numbers of large Eratosthenian and Copernican craters, assuming a constant cratering rate.

A. Based on frequencies of craters at least 1 km in diameter. Copernicus and Tycho frequencies from fig. 12.4, absolute ages from table 13.2. Mare-basalt frequencies from table 11.1, absolute ages from tables 11.3 and 12.4. Curve a, constant cratering rate since 3.2 aeons ago, based on crater frequencies on Apollo 12 and 15 mare units. Point a′, intersection with 1.2-aeon age of Copernicus; point a″, intersection with 0.81-aeon age of Copernicus (Eberhardt and others, 1973b; Alexander and others, 1976). Curve b, varying cratering rate since 3.2 aeons ago, passing through midpoint of Copernicus age. Curve c, constant cratering rate since 3.2 aeons ago, passing through midpoint of Copernicus age.

B. Based on D_L values. Copernicus and Tycho values from table 12.3 and Moore and others (1980b); mare-basalt values from table 11.1. Absolute ages as in *A*. Curve a, constant cratering rate since 3.2 aeons ago, based on average of Apollo 12 and 15 D_L values. Curve b, varying cratering rate since 3.2 aeons ago, drawn through midpoint of Copernicus age. Curve c, one of many possible curves representing D_L values on crater substrates (compare fig. 12.8).

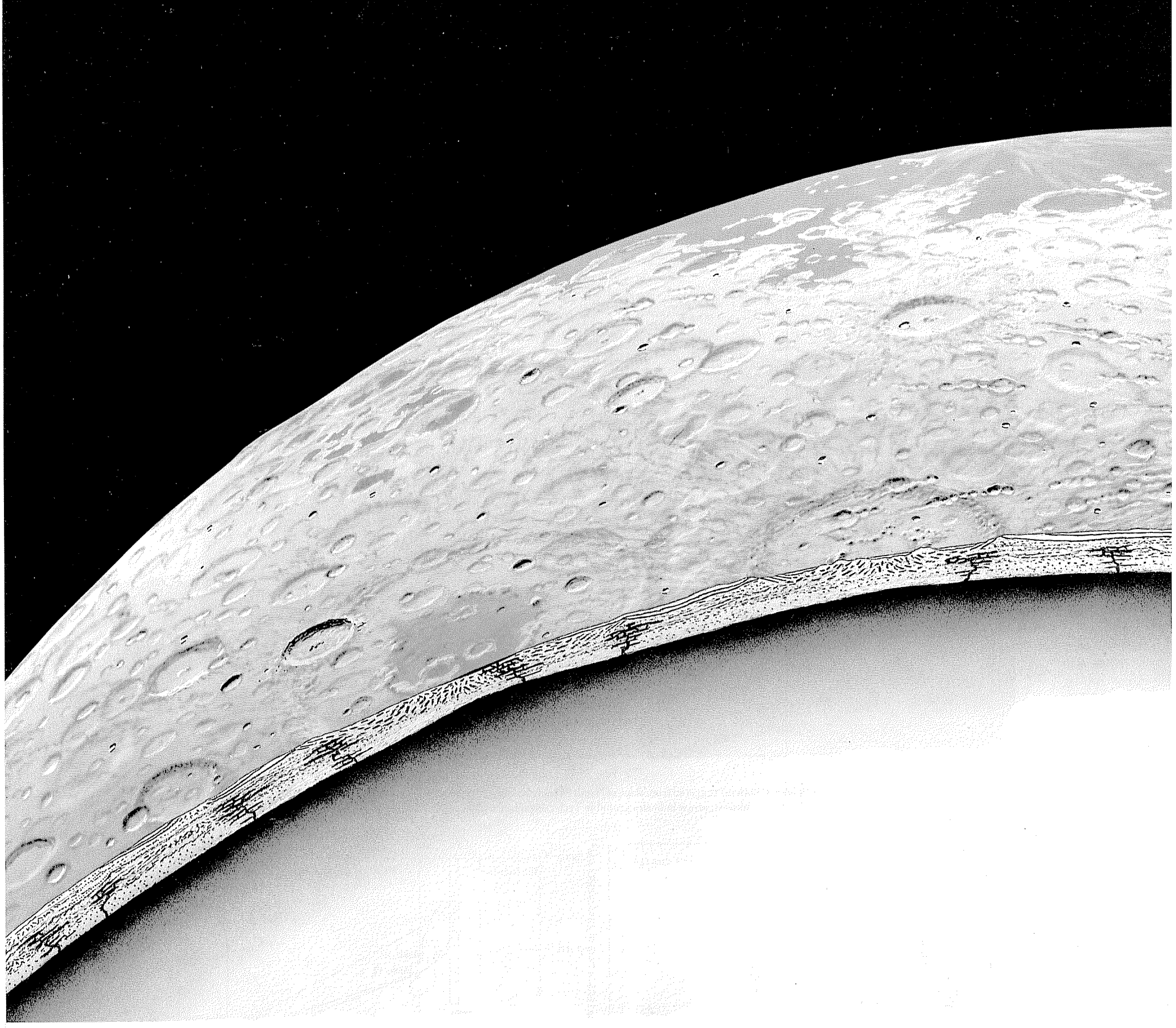

FIGURE 14.1.—Representative area of lunar surface (composite of several regions) and inferred subsurface structure. Mare basalt, gray in plan view and black in cross section, overlies impact melt in basins. Basin and crater ejecta blankets (white in cross section) overlap in several places, in accord with superposed-crater densities and degradational morphologies of surface exposures. Deformation of crustal material beneath basin rings is shown in accord with model in chapter 4; crust is thin, and mantle correspondingly uplifted, beneath basins. Stippling denotes possible unstratified lower crust that may have been reached only by the very largest impacts. True curvature; no vertical exaggeration. Painting by Donald E. Davis, courtesy of the artist.